An Adaptive Soft Computing Model for Flux Estimation and Torque Control of Induction Motors

Adel H Alshatti*
*(Department of Electrical Engineering, Shuwaikh Institute, PAAET, Kuwait.
Email: ah.alshatti@paaet.edu.kw)

ABSTRACT
Induction motors are widely utilized in various industries because of simplicity in service, durability, and low cost, leading to the displacement of DC motors. However, control system challenges have hindered their full potential for high performance. Many low-performance drives utilize scalar control, which adjusts only the stator magnitudes to uphold a persistent stator flux. Vector control emerged to address this limitation by enabling induction motor control analogous to DC motors. Subsequently, Direct Torque Controlled (DTC) induction motor drives were developed. Unlike vector-controlled drives where stator currents serve as control variables, DTC controls stator flux linkages. DTC employs a Reference Flux (RF) estimator to determine RF based on motor speed and a PI controller to estimate reference torque using speed error as input. The calculated stator flux angle determines the sector number for generating switching signals, traditionally done through a RF estimator. This estimator has been enhanced with fuzzy logic to ensure adaptability, and further improved with an ANFIS-based approach to combine fuzzy logic and artificial neural networks. Performance evaluation involves metrics utilizing speed and torque errors to gauge controller effectiveness. Comparing the fixed RF estimator to the ANFIS-tuned RF estimator with manually tuned speed PI, there is a performance improvement of 72.73%, 72.749%, and 46.636% for ISE, ITSE, and ITAE, respectively.
Keywords **-** Direct torque controller, reference flux, induction motor, ANFIS, vector controller.

I. INTRODUCTION

Direct Torque Control (DTC) based drives for induction motor offer numerous advantages in industrial applications, characterized by their simplicity and resilience to machine parameter variations, ensuring rapid response times. However, they are not without drawbacks, such as variable switching frequency and torque ripples stemming from imprecise voltage vectors for stator flux linkage generation. To mitigate these ripples and enhance performance, several approaches have been devised. One strategy involves refining the comparator within the DTC framework. Modifications made on torque hysteresis comparator can include adjusting the hysteresis band or increasing the number of levels, necessitating corresponding adjustments to the lookup table [1]. Additionally, optimizing sector division by expanding the number of sectors can further refine performance. Another widely adopted method is Space Vector Pulse Width Modulation (SVPWM), which offers significant improvements in DTC drive performance.

Artificial intelligence (AI) techniques are extensively applied in induction motor drives to enhance their performance. Unlike traditional methods, AI-based control strategies bypass the need for precise mathematical models to manage system nonlinearities and uncertainties. Key AI methodologies employed in DTC induction motor drives include fuzzy logic, artificial neural network (ANN), and artificial neuro-fuzzy systems (ANFIS). In the realm of DTC research, significant focus lies on Reference Flux (RF) estimation and reference torque estimation, crucial for calculating flux and torque errors respectively. Consequently, this study delves into investigating and refining these areas of interest within the DTC framework. Furthermore, to bolster performance, the research explores methods for adjusting the sector alteration of stator flux linkage [2]. This includes developing both fixed-angle and fuzzy-based angle approaches to optimize sector allocation.

DTC serves as an advanced controller scheme, focusing on the direct manipulation of two critical parameters such as torque and stator flux. Unlike traditional controllers, DTC does not rely on complex mathematical models or extensive calculations. Instead, it utilizes a hysteresis control approach to monitor and adjust torque and flux errors in real-time. The essence of DTC lies in its ability to not only regulate the magnitude but also the spatial position of the stator flux. By directly controlling these parameters, DTC ensures precise

and efficient motor operation. In practical implementation, the control algorithm continuously evaluates the torque and flux errors. These errors represent the disparities between the desired and actual values of torque and flux. To maintain these errors within acceptable bounds, DTC employs hysteresis comparators. These comparators generate control signals according to the deviation of flux and torque with respect to reference values. Moreover, DTC considers the spatial orientation of the stator flux, further refining its control strategy. By monitoring the position of the stator flux, the control system can adjust the switching signals sent to the inverter [3]. These signals dictate the operation of the inverter, which, in turn, determines the voltage applied to the motor.

The primary objective of DTC is twofold: to achieve rapid response times and minimize switching frequency. By constraining torque and flux errors within predefined hysteresis bands, DTC ensures swift and precise control while minimizing the number of switching events. This not only enhances motor performance but also reduces stress on the power electronics components, prolonging their lifespan [4]. To provide a visual representation of the spatial vectors involved in DTC, Fig. 1 illustrates the relationship between flux and current vectors within the induction machine. This graphical depiction aids in understanding the complex interplay of electrical parameters and their impact on motor performance.

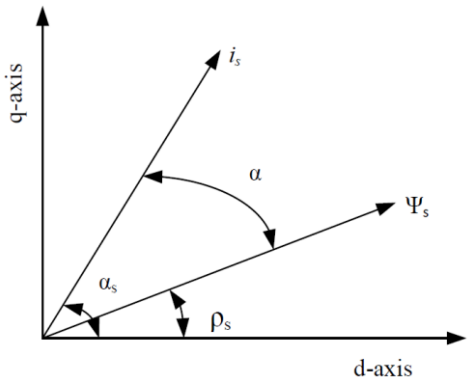

Fig. 1: Space vectors of flux and current in induction machine

In the case of 3-phase induction motor, Equation 1 defines the real time stator flux angle, while Equation 2 governs the electromagnetic torque.

$$\alpha = \alpha_s - \rho_s \tag{1}$$

$$T_e = \frac{3P}{4}|\varphi_s||i_s|\sin\alpha \tag{2}$$

Here, P indicates the pole count, φ_s represents the flux linkage in stator, i_s signifies the current space vector of stator, and α_s denotes the angle between the stator flux linkage and stator current space vectors. It's noteworthy that by maintaining the modulus of φ_s constant and manipulating the angle α_s, control over electromagnetic torque can be achieved. This implies that by applying stator voltages to the induction motor to uphold constant stator flux magnitude while rotating the position of φ_s, torque control is swiftly achieved. Through selecting an appropriate stator voltage from the inverter, both stator flux and electromagnetic torque can be effectively managed. This fundamental principle underpins the DTC of IM drives, wherein φ_s is directly influenced by the stator voltage source inverter. Neglecting the resistance of stator, the impact of inverter voltage on stator flux can be simplified, as represented by Equation 3.

$$V_s = \frac{d\varphi_s}{dt} \tag{3}$$

The flux plot is segmented into six sectors, labeled as α(1) through α(6). Sector 1, denoted as α(1), spans from -300 to 300. Similarly, sector 2, α(2), covers the range from 300 to 900, and this segmentation pattern continues up to sector 6. Non-zero voltage space vectors are employed to swiftly alter stator flux linkage space vectors. Conversely, zero voltage space vectors do not induce movement in stator flux linkages, albeit the voltage drop across the stator resistance prompts a gradual shift. In Figure 2, V1(100) through V6(101) represent voltage space vectors, while V0(000) and V7(111) depict the zero voltage space vectors.

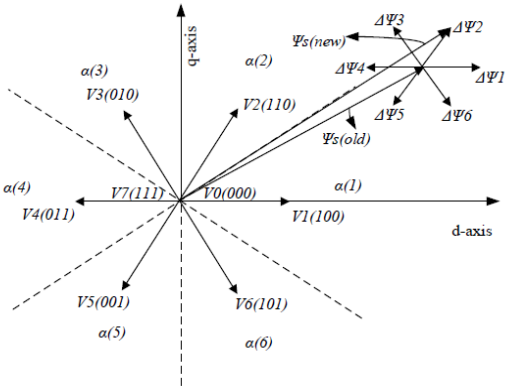

Fig. 2: Voltage vectors and stator flux linkage

Within the framework of DTC, effective control over stator flux linkage is achieved through meticulous selection of voltage space vectors [5]. The torque and flux are independently regulated by manipulating the tangential and radial components of φ_s. In DTC drives, the switching vectors (representing voltage space vectors) dispatched to the inverter are carefully chosen to ensure that the errors remain within their respective hysteresis bands throughout each sampling period.

II. LITERATURE SURVEY

Numerous researchers have contributed to the development of DTC-based induction motor drives, offering diverse control strategies to mitigate ripple and enhance speed control. A comprehensive literature review was undertaken to identify optimal methods for enhancing DTC drive performance, examining the evolution of DTC drive systems and available control strategies. Bassem et al. [6] focused on synthesizing two vector selection tables using a bus-clamping technique. This technique aimed to facilitate both clockwise and counterclockwise rotations of the induction motor. A comparative analysis was conducted between the proposed bus-clamping technique and a five-level torque-controlled DTC approach. Results demonstrated that the bus-clamping technique effectively reduced harmonic distortion, highlighting its potential for improving drive performance.

Taheri *et al.* [7] devised a flux search controller employing an adaptive gradient descent method to determine flux values in a six-phase induction machine DTC model. This optimization algorithm efficiently identifies the optimal flux value, ensuring swift performance. Brahim *et al.* [8] proposed the integration of a shunt resistor for measuring dc-link current in DTC setups. This measured current is utilized to reconstruct phase currents and voltages, enabling accurate estimation of motor flux and electromagnetic torque. Additionally, they implemented a zone shifting sector strategy and introduced a modified lookup table featuring synthesized voltage vectors. Venkataramana *et al.* [9] developed control schemes utilizing space vector modulation for a three-level diode-clamped inverter. Recognizing the inadequacy of conventional PI controllers in DTC for three-level inverters, they replaced them with Mamdani-type fuzzy-2 controllers. Comparative analysis revealed that fuzzy-2 DTC outperformed conventional PI controller DTC, showcasing its superior performance.

Pandit *et al.* [10] devised an algorithm for voltage vector selection based on virtual voltage vectors. These virtual vectors were instrumental in minimizing torque ripple through the utilization of five-level torque comparators. These techniques were specifically tailored for DTC applications in an asymmetrical six-phase induction motor setup. Nikzad *et al.* [11] employed a model predictive control approach to determine suitable voltage vectors for reducing flux and torque errors. Their method involved the incorporation of zero voltage vectors with available options to achieve accurate voltage vectors with varying duty cycles. Korkmaz *et al.* [12] explored the impact of artificial neural networks (ANN) on DTC performance. They developed, trained, and tested two distinct ANN models. The first model focused on identifying the flux sector region process, while the second model determined switching states based on data from flux hysteresis, torque hysteresis, and flux region outputs. Ibrahim *et al.* [13] proposed a constant switching frequency controller (CSFC) to regulate stator flux in DTC induction motor drives. This involved replacing the three-level torque hysteresis comparator with CSFC. Additionally, they employed an extended Kalman filter for estimating stator and rotor fluxes as well as motor speed.

Sampath *et al.* [14] introduced sliding mode control, a method that employs high-frequency switching to manipulate system states along a predefined hypersurface. While this approach is relatively straightforward in electric drives equipped with controlled on-off power converters, it does introduce challenges, particularly in the form of high-frequency chattering. In sliding mode control, continuous functions define the control surface, and discontinuous control actions are applied to guide the system towards a desired trajectory.

To mitigate the effects of chattering, a boundary layer is introduced in the switching surface. This boundary layer helps dampen the rapid oscillations associated with discontinuous control actions. Additionally, further enhancements have been made through the integration of a fuzzy logic controller, resulting in a hybrid approach known as fuzzy sliding mode control (FSMC). By combining the robustness of sliding mode control with the adaptability of fuzzy logic, FSMC offers improved performance and smoother operation in dynamic systems.

III. MATERIALS AND METHOD

Artificial Intelligence (AI) controllers play a vital role in enhancing the performance of variable frequency drives. Leveraging AI, it becomes feasible to develop drive systems with capabilities akin to learning, recalling, and executing trained patterns. As discussed in earlier sections, fuzzy logic finds application due to its adeptness in handling nonlinearities and uncertainties in parameters, even without a precise mathematical model. The efficacy of a fuzzy logic controller and its performance heavily rely on the expertise within the domain. Achieving performance enhancements often involves meticulous trial-and-error processes, especially in rule base formation and membership function (MF) selection. Similarly, when opting for neural networks, acquiring the necessary data for training the network can pose significant challenges. Success in training neural networks demands rigorous efforts and substantial resources.

ANFIS based model, depicted in Fig. 3, amalgamates the benefits of both fuzzy logic and neural networks. It combines the linguistic-based knowledge representation of fuzzy logic with the data training capabilities of neural networks. This hybrid approach empowers the development of highly adaptive drive systems, leveraging the learning capabilities of neural networks while minimizing the need for extensive human intervention in fine-tuning fuzzy logic rule bases. In ANFIS, data training imparts intelligence to fuzzy logic through structured learning from neural networks. This enables ANFIS to replace the conventional fuzzy logic controller. Furthermore, in the context of DTC, ANFIS serves to provide RF, supplanting the role traditionally held by fuzzy logic.

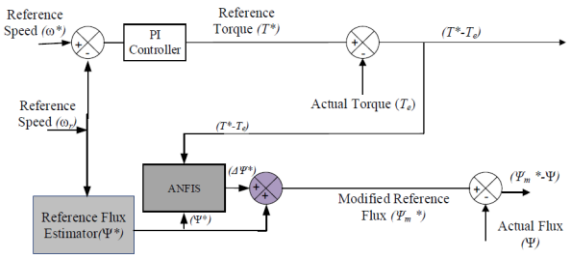

Fig. 3: ANFIS based estimator of RF

The ANFIS structure introduced for the DTC-IM drive is depicted in Fig. 4. Proposed configuration integrates a five-layered feedforward NN, incorporating multiple estimator techniques. Proposed model comprises the following layers: 1st layer serves as input layer. Fuzzy operation is carried out in the 2nd layer. The 3rd and 4th layers contain operational blocks responsible for controlling units. The 5th layer characterizes the de-fuzzy operation performed on the given data [15].

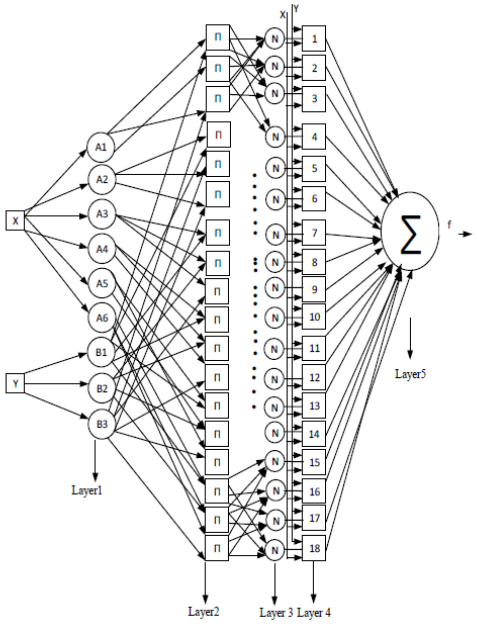

Figure 4: Proposed ANFIS structure

In the first layer in this work, two nodes are used for the torque error (T^*-T_e) and RF (φ^*). The inputs to the ANFIS structure under consideration are detailed here. Equations 4 and 5 depict the outputs generated by these layers. To alleviate computational load, geometrical MF has been selected for implementation within the proposed ANFIS [16].

$$O_{1,i} = \mu_{A1}(T^* - T_e) \quad (4)$$

$$O_{1,i} = \mu_{A2}(\varphi^*) \quad (5)$$

Within the 2nd layer, each node remains fixed. In this context, Equation 6 is utilized to estimate the input weights, aiming to minimize errors while considering the firing strength of the rules. Here, $\mu_{A1}(T^* - T_e)$ and $\mu_{A2}(\varphi^*)$ represent the degree of error and flux reference, respectively. Each node executes fuzzy AND as its node function.

$$O_{2,i} = \mu_i = \min\left[\mu_{A1}(T^* - T_e), \mu_{A2}(\varphi^*)\right] \quad (6)$$

In the 3rd layer, every node functions as a fixed node tasked with normalizing weights. In this layer, every node calculates the ratio of its assigned rule's firing strength to the total sum of firing strengths

across all rules. This computation yields the normalized value of firing strengths, as described by Equation 7.

$$O_{3,i} = \overline{\mu}_i = \frac{\mu_i}{\sum \mu_i} \quad (7)$$

Layer 4 comprises adaptive nodes, where the input MF and output are determined using a node function outlined in Equation 8. Within this equation, p_i, q_i, and r_i represent the parameters of node.

$$O_{4,i} = \overline{\mu}\left[p_i \mu_{A1}(T^* - T_e) + q_i \mu_{A2}(\varphi^*) + r_i \right] \quad (8)$$

In the 5th layer, a single fixed node handles the weighted output summation from layer 4. Equation 9 is utilized to compute the output from layer 5.

$$O_{5,i} = \sum \left[\overline{\mu}_i (f_i) \right] = \frac{\sum_i \left[\overline{\mu}_i (f_i) \right]}{\sum_i \mu_i} \quad (9)$$

In this study, the ANFIS network was trained using data obtained from the estimator. The data was applied into the ANFIS editor, and the model depicted in Fig. 4 was established. The five-layer network was then trained over 200 epochs using BPA with the provided input/output dataset. The toolbox constructed a fuzzy inference system (FIS), adjusting MF parameters through BPA. Subsequently, this ANFIS was integrated into existing systems and subjected to testing. MF underwent self-tuning to enhance overall performance.

IV. RESULTS AND DISCUSSIONS

The performance of various RF estimators, including conventional fixed, fuzzy, ANN, and ANFIS-based estimators are evaluated in thin section. The MATLAB/SIMULINK model substitutes the conventional reference estimator with a fuzzy-based one to enhance performance. Subsequently, ANN and ANFIS-based estimators are introduced for further improvement. The torque responses of each estimator are compared, focusing on a load torque of 3.65 Nm at 0.5 seconds. Figure 5 depicts the torque response in all cases. Notably, the conventional fixed RF estimator exhibits higher torque ripple amplitudes. However, as we progress from the fuzzy-based to the ANN and ANFIS-based estimators, torque ripples diminish gradually.

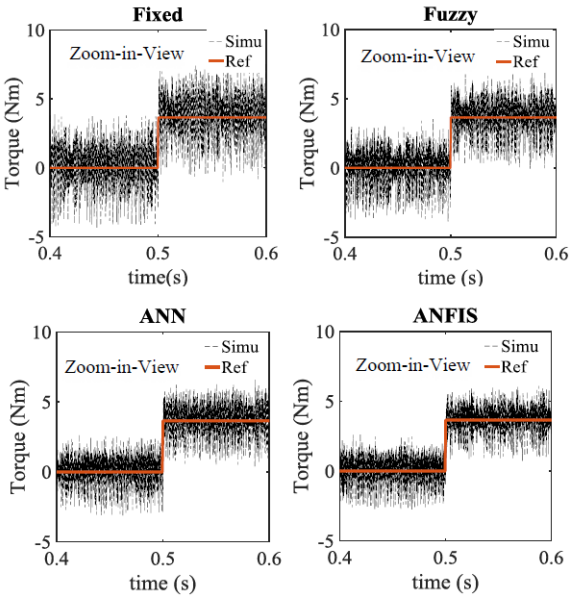

Fig. 5: Comparison of torque responses with a load of 3.65 Nm

Figure 6 illustrates the speed responses of different RF estimators, including the fixed, fuzzy-based, ANN-based, and ANFIS-based estimators, under a threshold speed of 138.54 rad/s. It is evident that ANFIS-oriented estimators closely track the reference speed compared to other estimators, even under a load of 3.65 Nm.

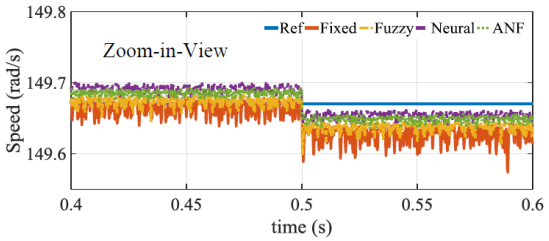

Fig. 6: Comparison of speed responses with a load of 3.65 Nm

In this study, the RF value dynamically adjusts in response to variations in the load. Consequently, the actual flux varies correspondingly. Fig. 7 presents a comparison among actual and RF responses for both fixed and variable RF estimators. The RF value of fuzzy system fluctuates between 0.6 Wb and 0.8 Wb, causing the actual flux to vary accordingly. For the ANN-system, the actual flux ranges from 0.58 Wb to 0.63 Wb, while in the proposed ANFIS model, it varies between 0.54 Wb and 0.59 Wb. Notably, when a step load is introduced at 0.5 s, the ANFIS-based RF estimator exhibits a lower requirement for actual flux. Across all four control strategies, the speed PI controller

maintains consistent gain values acquired through manual tuning.

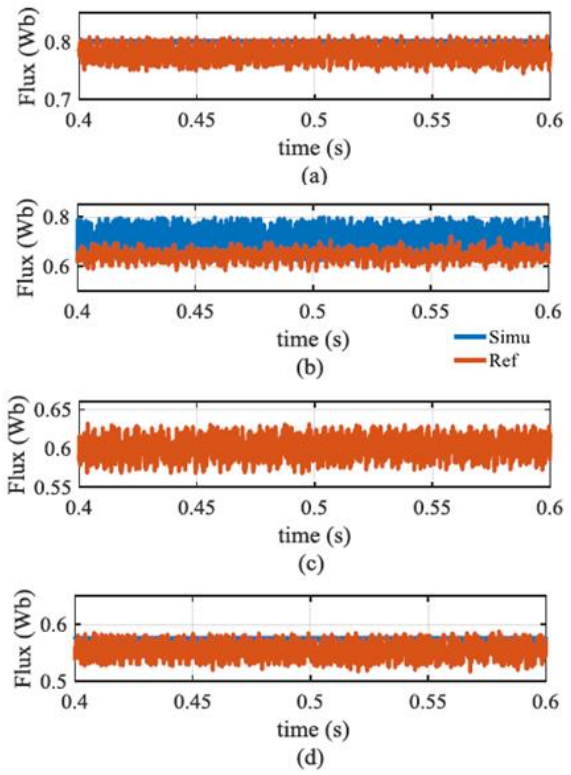

Fig. 7: Comparison of flux responses with a load of 3.65 Nm for (a) Fixed (b) Fuzzy (c) ANN (d) ANFIS

The optimal efficiency of a drive structure is computed by minimizing the value of a performance index. This index is quantified through Integral Square Error (ISE), Integral Time Absolute Error (ITAE), and Integral Time Square Error (ITSE), as defined in Equation (10), (11), and (12) respectively.

$$ISE = \int_0^{T_f} e(t)^2 dt \tag{10}$$

$$ITAE = \int_0^{T_f} t\,|e(t)|dt \tag{11}$$

$$ITSE = \int_0^{T_f} te(t)^2 dt \tag{12}$$

These indices serve as indicators of performance improvement achieved through the utilization of an ANFIS-model compared to a fuzzy-model in DTC. Table 1 presents the ISE values associated with the ANFIS-model. Control systems optimized to minimize ISE are effective at rapidly reducing large errors, encompassing both transient and steady-state behaviors. Therefore, evaluations based on ISE consider factors such as overshoot and rise time when assessing performance.

Table 1: ISE of ANFIS based flux estimator with manual tuning

Time	Torque	Flux	Speed
0.5 to 1s	0.834	0.0002760	0.000248
1 to 1.5s	1.920	0.0000652	0.009078
1.5 to 2s	1.209	0.0000680	0.001777
Total	3.963	0.0004092	0.011103

In the context of induction motor drive control, the primary objective frequently revolves around minimizing ITAE through controller parameter adjustments. Achieving this minimization results in faster settling time and reduced steady-state error, both highly desirable traits for numerous control applications. Table 2 presents the ITAE values associated with the ANFIS-model.

Table 2: ITAE of ANFIS model with manual tuning

Time	Torque	Flux	Speed
0.5 to 1s	0.3745	0.007750	0.00823
1 to 1.5s	0.8452	0.005598	0.08387
1.5 to 2s	1.0400	0.008081	0.05190
Total	2.2597	0.021429	0.14400

ITSE places a stronger emphasis on large errors compared to ITAE due to the squared error term, making it particularly responsive to significant deviations from the desired response. This sensitivity can be advantageous in specific control applications. Similar to ITAE, the aim in control system design frequently involves minimizing ITSE through controller parameter adjustments. Table 3 displays the ITSE values associated with the ANFIS-model.

Table 3: ITSE of ANFIS model with manual tuning

Time	Torque	Flux	Speed
0.5 to 1s	0.620	0.000206	0.000187
1 to 1.5s	2.274	0.000081	0.011320
1.5 to 2s	2.113	0.000119	0.003108
Total	5.015	0.000406	0.014615

The total ISE value for the fixed model with manually tuned PI speed controller is 0.084274, while for the ANFIS-model with manually tuned speed PI controller, it is 0.01728. Comparing these values, there is a percentage improvement from the fixed model to the fuzzy-model of 47.54%, 48.617%, and 13.913% for ISE, ITSE, and ITAE, respectively. Similarly, comparing the fixed reference model to the ANN-model with manually tuned speed PI, there is a performance improvement

of 72.73%, 72.749%, and 46.636% for ISE, ITSE, and ITAE, respectively. Therefore, it is evident that the ANFIS-model outperforms other estimators. Additionally, the percentage improvement of ANFIS-model with manually tuned speed PI controller in comparison to the fixed RF estimator with manually tuned speed PI controller is calculated as 79.2% for ITSE and 52.46% for ITAE. These results demonstrate that, akin to ISE values, ITSE and ITAE values also exhibit significant improvements.

V. CONCLUSION

This work delves into the significance of variable RF operation in enhancing the performance of induction motor drives. It introduces the concept of fuzzy-based variable RF estimation, detailing the development of MF for *Te* and conventional RF. Through analyses of responses and performance parameters, it is demonstrated that the proposed ANFIS estimator outperforms the conventional RF estimator in DTC induction motor drives. Furthermore, to further enhance performance, ANN and ANFIS-based RF models are introduced. By comparing the summation values of these estimators, it is evident that ANFIS achieves a reduction in ISE value of 74.4954%, while ANFIS achieves 72.3%, and Fuzzy achieves 47.54% compared to the conventional fixed RF estimator. Comparing the readings and error values, it is concluded that the ANFIS-based RF estimator emerges as the superior choice among fixed, fuzzy, and ANN-based RF estimators.

REFERENCES

[1] P. Chintan, P. P. Rajeevan, D. Anubrata, R. Rijil, K. Gopakumar and P. K. Marian, PK, "Fast direct torque control of an open-end induction motor drive using 12-sided polygonal voltage space vectors," *IEEE Transactions on Power Electronics*, vol. 27, no. 1, pp. 400-410, 2012.

[2] K. T. Orlowska, G. Tarchala and Dybkowski, "Sliding-mode direct torque control and sliding-mode observer with a magnetizing reactance for the filed-weakening of the induction motor drive," *Mathematics and Computers in Simulation*, vol. 98, pp. 31-45, 2019.

[3] K. Premalatha, S. Vasantharathna and S. Divyaah, "Self-excitation system for control of wind turbine driven induction generator using direct torque control," *Journal of Vibration and Control*, vol. 22, no. 3, pp. 736-755, 2021.

[4] M. N. Uddin, and M. Hafeez, "FLC- based DTC scheme to improve the dynamic performance of an IM drive," *IEEE Transactions on Industry Applications*, vol. 48, no. 2, pp. 823- 831, 2012.

[5] F. S. Tidjani, Hamadi, A. Chandra, A. Pillay and A. Vahdatifar, "Neural network based predictive DTC algorithm for induction motors," *International Journal of Electrical and Computer Engineering*, vol. 4, no. 11, pp. 1736-1740, 2010.

[6] E. B. Bassem, B. Badii, and M. Ahmed, "DTC scheme for a four-switch inverter-fed induction motor emulating the six-switch inverter operation," *IEEE Transactions on Power Electronics*, vol. 28, no. 7, pp. 3528-3538, 2013.

[7] T. Asghar, R. Abdolreza, and S. Kaboli, "Efficiency improvement in DTC of six-phase induction machine by adaptive gradient descent of flux," *IEEE Transactions on Power Electronics*, vol. 27, no. 3, pp. 1552-1562, 2012.

[8] M. Brahim, T. Nabil, B. Lotfi, R. Toufik, R and B. Seddik, "Low-cost direct torque control algorithm for induction motor without AC phase current sensors," *IEEE Transactions on Power Electronics*, vol. 27, no. 9, pp. 4132-413, 2012.

[9] N. Venkataramana Naik, Aurobinda Panda and S. P. Singh, "A three level fuzzy-2 DTC of induction motor drive using SVPWM," *IEEE transactions on Industrial Electronics*, vol. 63, no. 3, pp. 1467-1479, 2016.

[10] Jay K Pandit, Mohan V Aware, Ronak V Nemade and Emil Levi, "Direct torque control scheme for six-phase induction motor with reduced torque ripple," *IEEE Transactions on Power Electronics*, vol. 32, no. 9, pp. 7118-7129, 2017.

[11] M. R. Nikzad, Behzad Asaei S. O. Ahmadi, "Discrete duty cycle method for direct torque control of induction motor drives with model predictive solution," *IEEE Transactions on Power Electronics*, vol. 33, no. 3, pp. 2317-2329, 2018.

[12] Faith Korkmaz, "Speed and torque control of an induction motor with ANN based DTC," *International Journal of Instrumentation and Control Systems*, vol. 7, no. 1, pp. 15-24, 2017.

[13] Ibrahim Mohd Alsofyani and N. R. N. Idris "Simple flux regulation for improving state estimation at very low and zero speed of a speed sensorless direct torque control of induction motor," *IEEE Transactions on Power Electronics*, vol. 31, no. 4, pp. 3027-3035, 2016.

[14] S. Sampath Kumar, R. Joseph Xavier, and S. Balamurugan, "Speed control of DTC with torque ripple and flux droop reduction using sector alteration based adaptive sliding mode control," *Asian Journal of Information Technology*, vol. 15, no. 20, pp. 4020-4029, 2016.

[15] M. Hafeez, M. Nasir Uddin, N. A. Rahim, and W. P. Hew, "Self-tuned NFC and adaptive hysteresis-based DTC scheme for IM drive," *IEEE Transactions on Industry Applications*, vol. 50, no. 2, pp. 1410-1420, 2014.

[16] Fayez G Areed, Amira Y Haikal and Reham H Mohammed, "Adaptive neuro-fuzzy control of

induction motor," *Ains Shams Engineering Journal*, vol. 1, no. 1, pp. 71-78, 2010.